Evidence for the Involvement of Ala 166 in Coupling Na^+ to Sugar Transport through the Human Na^+/Glucose Cotransporter†

Anne-Kristine Meinild, Donald D. F. Loo,* Bruce A. Hirayama, Elsa Gallardo, and Ernest M. Wright

Department of Physiology, University of California at Los Angeles School of Medicine, Los Angeles, California 90095-1751

Received May 18, 2001; Revised Manuscript Received July 27, 2001

ABSTRACT: We mutated residue 166, located in the putative Na^+ transport pathway between transmembrane segments 4 and 5 of human Na^+/glucose cotransporter (hSGLT1), from alanine to cysteine (A166C). A166C was expressed in *Xenopus laevis* oocytes, and electrophysiological methods were used to assay function. The affinity for Na^+ was unchanged compared to that of hSGLT1, whereas the sugar affinity was reduced and sugar specificity was altered. There was a reduction in the turnover rate of the transporter, and in contrast to that of hSGLT1, the turnover rate depended on the sugar molecule. Exposure of A166C to MTSEA and MTSET, but not MTSES, abolished sugar transport. Accessibility of A166C to alkylating reagents was independent of protein conformation, indicating that the residue is always accessible from the extracellular surface. Sugar and phlorizin did not protect the residue from being alkylated, suggesting that residue 166 is not located in the sugar pathway. MTSEA, MTSET, and MTSES all changed the pre-steady-state kinetics of A166C, independent of pH, and sugars altered these kinetics. The inability of MTSEA-labeled A166C to transport sugar was reversed (with no major change in Na^+ and sugar affinity) if the positive charge on MTSEA was neutralized by increasing the external pH to 9.0. These studies suggest that the residue at position 166 is involved in the interaction between the Na^+ and sugar transport pathways.

Ion-driven cotransport proteins couple the electrochemical potential gradient for ions (Na^+ and H^+) to the uphill transport of substrates (sugars, amino acids, neurotransmitters, osmolytes, vitamins, ions, and water). For the Na^+/glucose cotransporter (SGLT1),[1] Na^+ is an essential activator, binding to the transporter before glucose (*1*, *2*). SGLT1 is a monomer with 14 transmembrane segments (TMS) (*3*, *4*). Functional analysis of SGLT1 chimeras and truncated proteins has indicated that the sugar permeation pathway is composed of the C-terminal 5 TMS (*5*, *6*). The N-terminal half of SGLT1 has been proposed to be involved in Na^+ permeation; mutagenesis of residues in the N-terminus of SGLT1 has resulted in alterations in cation binding (*7*−*9*). It was found recently that amino acid residue Asp 204, localized on the intracellular side of the membrane within the Na^+ transport pathway, is involved in the cation selectivity of the transporter (*7*).

In our studies of mutations in human SGLT1 (hSGLT1) that cause glucose−galactose malabsorption (GGM), we have found several missense mutations in the N-terminal half of the protein that cause defects in sugar transport (*10*). One of these, A166T, reduced sugar transport 90%, and this was largely due to a trafficking defect. Following our success in restoring transport of GGM mutants by cysteine mutagenesis, e.g., Q457R to Q457C (*2*), and studies of A166C in rabbit SGLT1 (*8*, *9*, *11*), we decided to characterize the properties of the hSGLT1 A166C mutation. Another motivation for reexamining A166C is our finding that the external hydrophilic loop between TMS 4 and 5 containing residue 166 is within 8 Å of the sugar translocation pathway (*12*). This proximity raises the possibility that residue 166 is involved in interactions between the Na^+ and sugar transport pathways of the protein. We expressed A166C in *Xenopus laevis* oocytes and examined the steady-state and pre-steady-state kinetics and sugar specificity before and after alkylation of A166C with methanethiosulfonate (MTS) reagents. Although our studies confirm and extend the previous reports on the rabbit SGLT1 A166C mutation, our interpretation of the results diverges significantly from those of Silverman's group (*8*, *9*). We propose that interactions between residue 166 and the sugar binding/translocation pathway are involved in determining sugar selectivity and transport.

EXPERIMENTAL PROCEDURES

Molecular Biology and Expression in Oocytes. Substitution of alanine with cysteine at residue 166 was performed by

† This research was supported by NIH Grants DK44582, DK19567, DK44602, GM52094, and GM99004, and a postdoctoral fellowship from the Carlsberg Foundation (A.-K.M.).

* To whom correspondence should be addressed: Department of Physiology, UCLA School of Medicine, 10833 LeConte Ave., Los Angles, CA 90095-1751. Phone: (310) 206-8569. Fax: (310) 206-5886. E-mail: dloo@mednet.ucla.edu.

[1] Abbreviations: SGLT1, Na^+/glucose transporter; WT, wild-type human SGLT1; TMS, transmembrane segment; GGM, glucose−galactose malabsorption; V_h, holding membrane potential; V_t, test potential; I_{max}, maximal substrate-induced current; $K_{0.5}$, half-maximal substrate concentration; n, Hill coefficient; τ, relaxation time constant; τ_{max}, maximal time constant; Q_{max}, maximum charge; $V_{0.5}$, membrane potential at 50% Q_{max}; z, apparent valence of the movable charge; $\boldsymbol{Q}_{+50}$, charge transfer at +50 mV; τ_{+50}, relaxation time constant at +50 mV; I^{sugar}, sugar-induced current; D-Gal, D-galactose; D-Glu, D-glucose; α-MDG, α-methyl D-glucopyranoside; MTS, methanethiosulfonate; MTSEA, (2-aminoethyl)methanethiosulfonate hydrobromide; MTSES, sodium(2-sulfonatoethyl)methanethiosulfonate; MTSET, [2-(trimethylammonium)ethyl]methanethiosulfonate bromide.

10.1021/bi011026l CCC: $20.00
Published on Web 09/08/2001

site-directed mutagenesis, using the two-step polymerase chain reaction protocol (*13*). The plasmid encoding wild-type hSGLT1 (WT) cDNA was used as a template. WT and A166C encoding plasmids were linearized with *Xba*I and in vitro transcribed into cRNA from the T3 promoter (MEGA-script kit, Ambion, Austin, TX). *X. laevis* oocytes were defolliculated, injected with 50 ng of cRNA, and maintained in Barth's medium supplemented with 50 mg/mL gentamycin at 18 °C for 3−8 days before being used (*1*).

Electrophysiological Methods. The two-electrode voltage clamp method was used to control the membrane potential and monitor cotransporter activity as previously described (*2, 14*). The oocytes were normally bathed in a NaCl buffer [100 mM NaCl, 2 mM KCl, 1 mM $CaCl_2$, 1 mM $MgCl_2$, and 10 mM HEPES-Tris (pH 7.5)] with the membrane potential held at −50 mV. All experiments were performed under continuous perfusion of the chamber. The steady-state sugar-induced current was the difference in current before and after addition of sugar [methyl α-D-glucopyranoside (α-MDG), D-glucose (D-Glu), or D-galactose (D-Gal)] to the NaCl buffer. Na^+ free solutions were prepared by substituting choline chloride for NaCl in the NaCl buffer. For solutions buffered at pH 9.0, the HEPES was replaced with CAPS [3-(cyclohexylamino)propanesulfonic acid].

For steady-state kinetic analysis, the steady-state sugar-induced current (I^{sugar}) was measured at different membrane voltages. At each voltage, I^{sugar} versus substrate concentration relations were fitted to eq 1

$$I = I_{max}[S]^n/([S]^n + K_{0.5}{}^n) \quad (1)$$

where [S] is the external concentration of the substrate (Na^+ or sugar), I_{max} is the maximal current for saturating [S], $K_{0.5}$ is the half-maximal substrate concentration (or the apparent affinity constant), and n is the Hill coefficient. Sugar activation of A166C was studied at 100 mM external Na^+ by varying the sugar concentration, and Na^+ activation was studied at a fixed (saturating) sugar concentration by varying the external Na^+ concentration.

The pre-steady-state transient currents of A166C were isolated using the phlorizin-subtraction method (*14*). The oocyte was bathed in NaCl buffer, and the membrane potential was held at −50 mV. The membrane potential was jumped to a series of test values (V_t, ranging from +50 to −150 mV with 20 mV increments) for 30 ms before returning to the holding potential (V_h). The pulse protocol was repeated with addition of a saturating concentration of the SGLT1 inhibitor phlorizin (100 μM) to the external solution. At each test potential, SGLT1 pre-steady-state transient currents were obtained by subtraction of the current relaxations in phlorizin from those obtained in the absence of phlorizin. The relaxation time constants were obtained by fitting the A166C transient currents to a single exponential

$$I = I_1 e^{-t/\tau_1}$$

where I is the A166C transient current with initial amplitude I_1 and time constant τ_1, and t is the time from the onset of the voltage pulse. The charge movement, Q, was obtained by integrating the transient currents at different potentials with respect to time. The charge−voltage (Q/V) relations were fitted to a Boltzmann function

$$(Q - Q_{hyp})/Q_{max} = 1/\{1 + \exp[z(V_t - V_{0.5})F/RT]\}$$

where $Q_{max} = Q_{dep} - Q_{hyp}$ (Q_{dep} and Q_{hyp} are Q at depolarizing and hyperpolarizing limits, respectively), F is the Faraday constant, R is the gas constant, T is the absolute temperature, $V_{0.5}$ is the membrane potential where there is 50% charge transfer, and z is the apparent valence of the movable charge (*14*).

Treatment with Methanethiosulfate Reagents. MTS reagents ($MTSEA^+$ [(2-aminoethyl)methanethiosulfate], $MTSET^+$ {[(2-trimethylammonium)ethyl]methanethiosulfate}, and $MTSES^-$ [(2-sulfonatoethyl)methanethiosulfate]) were freshly prepared and used as described previously (*2*). Prior to treatment with the MTS reagents, transporter activity was measured as the sugar-induced current at a saturating sugar concentration and a V_h of −50 mV. MTS treatment was performed by adding the MTS reagent to the superfusing solution for a desired time, solution composition, and membrane potential. The MTS reagent was washed out of the chamber, and the membrane potential was returned to V_h. The extent of alkylation was determined from the residual sugar-dependent current. In the case of MTSES, the extent of alkylation was determined as the protection from subsequent alkylation with MTSEA or MTSET (see below).

Transport Assay. Na^+-dependent sugar uptake was carried out as described by Ikeda et al. (*15*). The initial rate of sugar uptake into five to seven oocytes was measured at 22 °C using radioactive [U-^{14}C]glucose (250 mCi/mmol, ICN Biomedicals, Inc.) at a final concentration of 50 μM in either NaCl buffer or choline buffer. Na^+-dependent uptake was the difference in uptake in NaCl and choline buffer.

All of the experiments were performed on two to five oocytes from different donor frogs unless otherwise noted. Statistics are given as means ± standard error, and n is the number of experiments; in cases where data were obtained from estimates using equations, the statistics are expressed as the standard errors of the fits.

RESULTS

The A166C mutant was functionally expressed in oocytes. Figure 1A is an example of a current record from an oocyte expressing A166C with the membrane potential held at −50 mV. When a saturating concentration (100 mM) of either α-MDG, D-Glu, or D-Gal was added to the superfusing NaCl buffer, they all induced inward currents, I^{sugar}, but with different magnitudes: $I^{D-Gal} > I^{D-Glu} \gg I^{\alpha-MDG}$. Figure 1B shows the steady-state I/V relationship of the Na^+/sugar currents. The Na^+/sugar currents increased as the membrane potential was hyperpolarized, but did not saturate, in contrast to those of wild-type hSGLT1. The I/V relationships of glucose-induced currents are compared for WT and A166C in Figure 1C.

In the absence of sugar, A166C exhibited a Na^+ leak (uniport) current (I_{leak} in Figure 1B), as determined by subtraction of the current with 100 μM phlorizin added to the external solution from the current in the NaCl buffer. The Na^+ leak current saturated with hyperpolarizing potentials and was 5 ± 2% of the Na^+/glucose current at −150 mV.

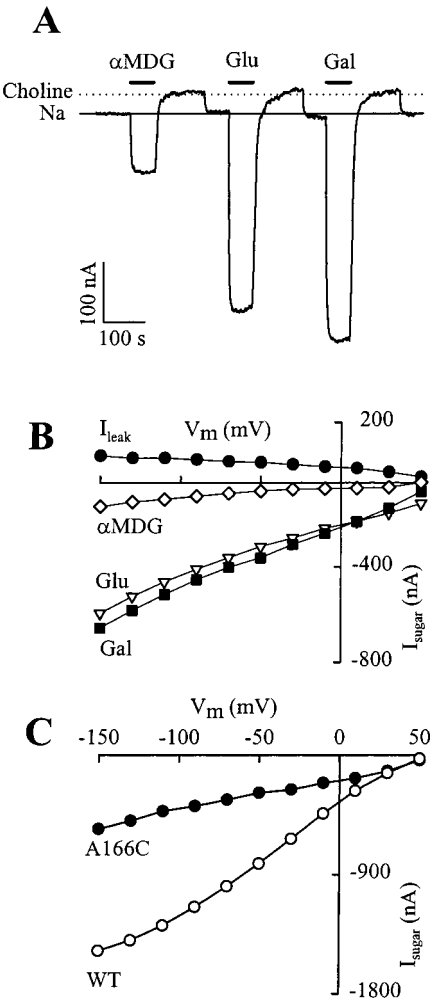

FIGURE 1: Na^+ currents mediated by an A166C-expressing oocyte. (A) Chart recording of whole-cell current under voltage clamp conditions. The oocyte was initially superfused with Na^+ buffer and the membrane clamped at −50 mV. The current was monitored continuously as the bath solution was changed. Addition of 100 mM sugar to the bathing solution generated an increase in inward current (I^{sugar}). I^{sugar} was −95 nA for α-MDG, −335 nA for D-Glu, and −375 nA for D-Gal. After wash-out of the sugar with choline buffer, the current returned to the baseline holding value. The solid line indicates the holding current in Na^+ and the dashed line the current in choline. (B) *I*/*V* curves of Na^+ currents. Steady-state substrate-induced currents ($I = I^{substrate} - I^{Na}$) were obtained for voltages from +50 to −150 mV. The oocyte was bathed in Na^+ buffer, and the change in current was recorded for each voltage after addition of 100 mM D-Gal (■), D-Glu (▽) α-MDG (◇), or 100 μM phlorizin (Na^+ leak current I_{leak}) (●) and plotted as a function of *V*. The scale on the voltage axis in panel B is the same as that in panel C. (C) Steady-state currents induced by 100 mM D-Glu measured for A166C (●) and WT (○) and plotted as function of *V*, ranging from +50 to −150 mV.

Steady-State Kinetics. The kinetics of sugar transport were determined by measuring the steady-state Na^+/sugar currents as a function of external sugar concentration at a constant Na^+ concentration (100 mM). The values for the maximal transport rate, I_{max}, and $K_{0.5}^{sugar}$ at a membrane potential of −150 mV are shown in Figure 2. In the same oocyte, the I_{max} was different for each sugar. D-Gal induced the largest inward current, whereas D-Glu and α-MDG induced currents that were 85 ± 4 and 21 ± 1% of that of D-Gal (Figure 2A). There was a difference in $K_{0.5}^{sugar}$ for the sugars: $K_{0.5}^{D-Gal} = 5.4 \pm 0.2$ mM, $K_{0.5}^{D-Glu} = 1.5 \pm 0.1$ mM, and $K_{0.5}^{\alpha-MDG} = 1.7 \pm 0.1$ mM (Figure 2B). For each of the three sugars, $K_{0.5}^{sugar}$ was independent of membrane voltage from −50 to −150 mV.

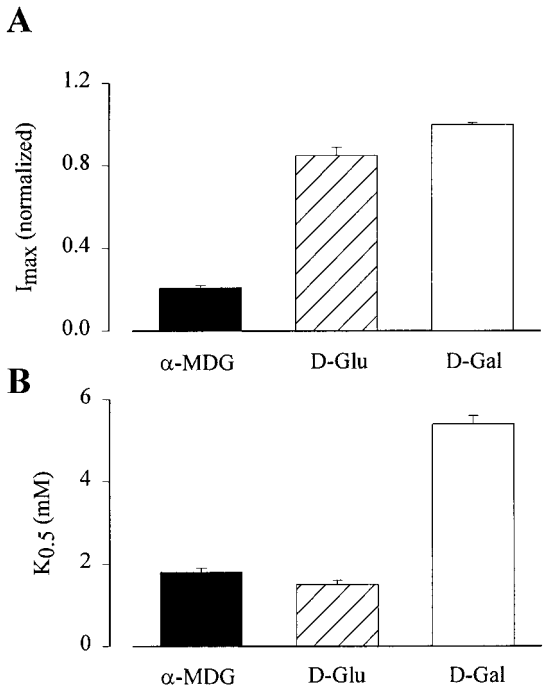

FIGURE 2: Kinetics of sugar transport. The sugar concentration was varied from 0 to 100 mM while the Na^+ concentration was maintained at 100 mM, and sugar-induced currents as a function of the sugar concentration were fitted to eq 1 to derive values for I_{max} and $K_{0.5}^{sugar}$. (A) I_{max} for the sugars at −150 mV normalized to the maximal transport rate in D-Gal. Normalized I_{max} was 0.24 ± 0.01 for α-MDG, 0.81 ± 0.01 for D-Glu, and 1 ± 0.01 for D-Gal. (B) $K_{0.5}^{sugar}$ at −150 mV was 1.8 ± 0.3 mM for α-MDG, 1.5 ± 0.1 mM for D-Glu, and 5.6 ± 0.2 mM for D-Gal. Data were obtained from two or three oocytes.

The kinetics of Na^+ transport were determined by measuring the steady-state Na^+/sugar currents as a function of external Na^+ concentration at saturating sugar (D-Gal or D-Glu). In contrast to $K_{0.5}$ for sugar, $K_{0.5}^{Na}$ was voltage-dependent. $K_{0.5}^{Na}$ was 0.9 ± 0.2 mM at −150 mV, 1.2 ± 0.1 mM at −110 mV, and 7.5 ± 0.6 mM at −30 mV. The Hill coefficient (*n*) was 2.0 ± 0.8 at −150 mV and was independent of voltage (not shown).

Pre-Steady-State Charge Movement. Figure 3A shows the pre-steady-state currents of A166C obtained by the phlorizin subtraction method. The membrane potential was held at −50 mV and stepped to test potentials from +50 to −150 mV. For both depolarizing and hyperpolarizing voltage pulses, the transient currents rose to a peak before decaying to the steady state. At each voltage, the charge movement (*Q*) was obtained by integration of the transient currents. *Q* plotted against the voltage gave a sigmoidal charge/voltage (*Q*/*V*) curve (Figure 3B). The maximal charge transfer, Q_{max}, varied between 34 and 77 nC, depending on the expression level of A166C. $V_{0.5}$ ranged from −3 to −12 mV, and *z* was ≈1. For comparison, the *Q*/*V* curve for WT is also shown in Figure 3B. For WT, $V_{0.5}$ was −36 ± 1 mV and *z* was 1.

Figure 3C shows the voltage dependence of the relaxation time constants, τ, for A166C and WT. For WT, τ was highly dependent on membrane voltage, with a maximum (τ_{max}) of

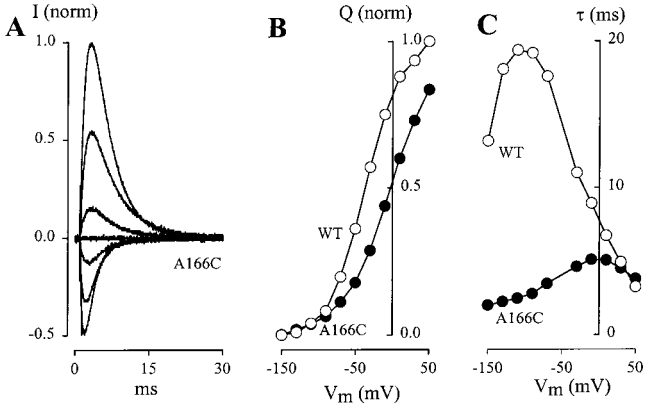

FIGURE 3: Comparison of A166C with wild-type hSGLT1. (A) Pre-steady-state current traces for A166C. Total currents were obtained as the membrane potential was held at −50 mV and stepped to test potentials, V_t (from +50 to −150 mV with 20 mV increments). Shown are the current records at V_t values of +50, +10, −30, −50, −70, −110, and −150 mV. Upward deflections of the current traces correspond to depolarizing potentials and downward deflections to hyperpolarizing potentials. Transporter specific transient currents were isolated by the phlorizin method (see Experimental Procedures). (B) Charge/voltage relationships for A166C and WT. Q_{max} was normalized to 1 and the Q/V curve fitted to the Boltzmann equation. WT (○) had a $V_{0.5}$ of −36 ± 1 mV, and for A166C (●), $V_{0.5}$ was −8 ± 3 mV. There was no difference in z (=1). (C) Voltage dependence of the relaxation time constant, τ, for WT (○) (τ_{max} = 20 ms, at −100 mV) and A166C (●) (τ_{max} = 5.5 ms, at $V_{0.5}$). WT data were taken from ref *7*.

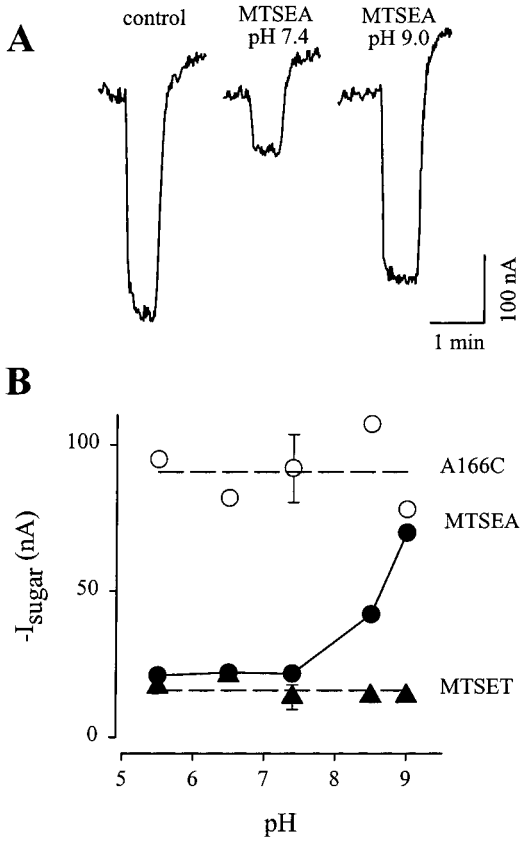

FIGURE 4: Effect of pH on sugar-induced currents after labeling with MTS reagents. (A) Effect on MTSEA at pH 7.4 and 9.0. An oocyte expressing A166C was clamped at −50 mV and the inward current measured continuously, while the composition and pH of the superfusing solution were changed. Before exposure to MTSEA, addition of 100 mM D-Glu to the Na^+ buffer (pH 7.4) induced a current of −330 nA. After the current returned to baseline, the oocyte was exposed to 1 mM MTSEA for 2 min (not shown). This resulted in a reduction of the sugar-induced current to −80 nA. At pH 9.0, the sugar-induced current recovered (−275 nA). (B) pH dependence of sugar-induced currents of A166C and A166C alkylated by MTSEA or MTSET. For alkylation, oocytes were exposed to 1 mM MTS reagent for 2 min. The membrane potential was held at −50 mV, while the sugar-induced currents were measured at different pHs for A166C (○), A166C alkylated by MTSEA (●), and A166C alkylated by MTSET (▲). For each pH value, an oocyte was perfused by a Na^+ buffer at the given pH, to give the baseline current. D-Gal (100 mM) was added to the solution, and the sugar-induced current was measured. This experiment was performed with one to three different oocytes from the same donor frog, and I^{sugar} (100 mM D-Gal at −50 mV) varied from −65 to −94 nA.

20 ms at −100 mV. In A166C, τ_{max} was much faster (5−6 ms) and shifted to ∼0 mV.

In the presence of sugar, charge movements associated with A166C were observed when membrane potential was stepped to depolarizing values. For example, analysis of pre-steady-state currents from one oocyte at the test potential of +50 mV gave charge transfers (Q_{+50}) of 11 nC and relaxation time constants (τ_{+50}) of 14 ms in D-Gal, 4 nC and 18 ms in D-Glu, and 8 nC and 6 ms in α-MDG. For the same oocyte in Na^+ buffer, Q_{+50} = 57 nC and τ_{+50} = 5 ms. The charge movement in sugar did not saturate at depolarizing potentials with the pulse protocol employed (V_h of −50 mV, V_t from +50 to −150 mV), whereas in Na^+ (in the absence of sugar), the charge movement was close to saturation at +50 mV (data not shown). In WT, no charge movement is observed at saturating sugar concentrations (*14*).

Accessibility of A166C to MTS Reagents. Alkylation of A166C by MTS reagents altered the function of the transporter. After treatment with MTSEA and MTSET (1 mM for 2 min), the inward sugar-induced current was inhibited by 78 ± 13% (n = 4, Figure 4A) and 94 ± 2% (n = 3), respectively. Treatment with MTSES (1 mM for 40 min) did not inhibit Na^+/glucose currents (not shown). In control experiments, treatment of WT with MTS reagents did not have any effect on sugar-induced currents (*2*).

The conformational states of SGLT1 have been shown to depend on the Na^+ and sugar concentrations and membrane voltage (*2*), and it is possible to test accessibility of a residue at different states by varying these conditions. For A166C, it was found that the accessibility of residue 166 to MTS reagents was independent of protein conformation. For example, the percentage inhibition of I^{sugar} after treatment with 1 mM MTSEA was 72% after a 2 min exposure in choline buffer at 0 mV, and 78% after treatment for 2 min in Na^+ buffer at −100 mV. Furthermore, sugar did not protect A166C from alkylation. When 1 mM MTSEA or MTSET was added to the external Na^+ buffer containing sugar, the inward currents were reduced to the same extent as in Na^+ buffer without sugar (not shown).

Effect of the Charge of the MTS Reagent. MTSET is positively charged at all pHs that were used, whereas the charge on MTSEA depends on the pH of the external medium and the pK_a of the amine, which has been reported to be ≥8.5 (*16*). At pH 7.4, the majority (>90%) of MTSEA is positively charged ($MTSEA^+$), and the compound is predominantly deprotonated (≈75%) to the neutral form ($MTSEA^0$) at pH 9.0. Figure 4A shows a current record (V_h was −50 mV) of an A166C-expressing oocyte before and after treatment with MTSEA (1 mM for 2 min, at −50 mV).

After MTSEA, the D-Glu-induced current was reduced 75% at pH 7.4, whereas at pH 9.0, the current recovered.

Reduction of the sugar-induced current in A166C treated with MTSEA was dependent on pH (Figure 4B). When D-Gal was tested at pH 9.0 ($MTSEA^0$), there was little inhibition of current. But as the pH was lowered, the sugar-induced current was gradually reduced by ~50% at pH 8.5, and by ~75% at pH 7.4. For both nontreated A166C and A166C treated with MTSET, the magnitude of the sugar-induced current was relatively insensitive to pH (Figure 4B).

The positive charge on MTSEA did not affect the ability of the reagent to react with A166C. After labeling with MTSEA at pH 9.0 (1 mM for 2 min, at −50 mV) where the positive charge is neutralized, the sugar-induced current was approximately the same. But when the pH was changed to 7.5, the sugar-induced current was reduced by ~75% (not shown).

When A166C was incubated in 1 mM MTSES for 1 h, there was no reduction in the sugar-induced current. However, after pretreatment with MTSES, subsequent exposure to 1 mM MTSET for 2 min reduced the sugar-induced current by only 57% compared to the 90% inhibition of A166C not pretreated with MTSES.

In WT, it is well established that the sugar-coupled current (I^{sugar}) is directly correlated with sugar uptake into the cell (*7*, *17*, *18*). To test whether I^{sugar} was correlated with sugar uptake in A166C, in parallel experiments we compared inhibition of D-Glu-induced currents and uptakes. In A166C-expressing oocytes treated with MTSET (1 mM for 5 min), I^{D-Glu} was reduced 83 ± 5% ($n = 4$), and Na^+-dependent D-[^{14}C]glucose uptake was reduced by ~90% ($n = 2$). For MTSES, there was no inhibition of I^{D-Glu} (89 ± 10%, $n = 4$) or D-[^{14}C]glucose uptake (93 ± 5%, $n = 3$). However, 45 ± 10% ($n = 4$) of the sites were alkylated (there was an only 56% reduction in I^{D-Glu} when MTSES-pretreated oocytes were exposed to 1 mM MTSET for 2 min).

Steady-State Kinetics after MTSEA Treatment. The kinetics of Na^+ and sugar transport were determined at pH 9.0 before and after MTSEA treatment. Compared to that of untreated A166C, the Na^+ affinity was decreased. On the same oocyte, when $K_{0.5}^{Na}$ values before and after treatment with MTSEA were compared (1 mM MTSEA for 2 min, at −50 mV), $K_{0.5}^{Na}$ was 0.8 ± 0.2 and 1.7 ± 0.2 mM at −150 mV, 1.9 ± 0.2 and 4.3 ± 0.2 mM at −90 mV, and 7.9 ± 0.7 and 11.5 ± 0.7 mM at −30 mV. For all three sugars (α-MDG, D-Glu, and D-Gal), there was little change in $K_{0.5}^{sugar}$ at −150 mV (at pH 9.0) before and after MTSEA treatment. On the same oocyte at −150 mV before and after treatment, $K_{0.5}^{\alpha-MDG}$ was 1.8 ± 0.3 and 2.6 ± 0.4 mM, $K_{0.5}^{D-Glu}$ was 1.4 ± 0.1 and 1.0 ± 0.2 mM, and $K_{0.5}^{D-Gal}$ was 4.6 ± 0.3 and 5.5 ± 0.2 mM. However at −30 mV, $K_{0.5}^{sugar}$ increased after MTSEA treatment. For α-MDG, $K_{0.5}$ increased from 4.6 ± 0.9 to 27.5 ± 14.5 mM, for D-Glu, from 2.1 ± 0.3 to 9.5 ± 0.8 mM, and for D-Gal, from 10 ± 0.7 to 54 ± 17 mM. These increases in $K_{0.5}$ for sugars are due, at least in part, to a decreased affinity for Na^+ (increased $K_{0.5}^{Na}$) at this voltage.

Pre-Steady-State Charge Movement after Treatment with MTS Reagents. Alkylation altered the pre-steady-state kinetics of A166C. All three MTS reagents had the same effect on A166C by shifting the distribution of the *Q*/*V* curve to more hyperpolarizing potentials (since MTSES reacted with only 50% of the sites, a full analysis of the pre-steady-state current traces was not performed). There was a shift in $V_{0.5}$ of approximately −15 mV for MTSEA and approximately −35 mV for MTSET (Figure 5A). The relaxation time constants were reduced, and the voltage at τ_{max} was shifted to more negative values. For MTSEA, τ_{max} was ≈3.4 ms and for MTSET, 1.5 ms, compared to a value of 5 ms for A166C (Figure 5B). Pre-steady-state kinetics after MTSEA treatment were independent of pH. On the same oocyte treated with MTSEA, $V_{0.5}$ was −20 mV at pH 7.4 and −19 mV at pH 9.0. τ_{max} was 4.3 ms at pH 7.4 and 3.9 ms at pH.9.0.

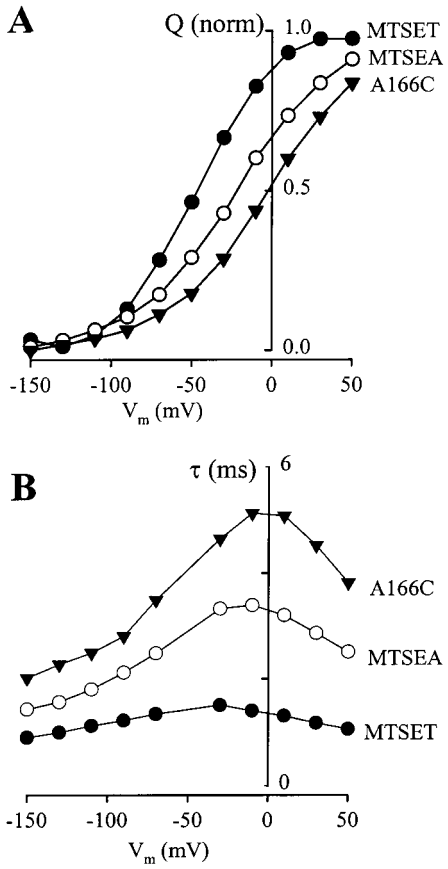

FIGURE 5: Effects of MTSEA and MTSET on $V_{0.5}$ and the transient current relaxation time constant, τ. (A) Charge/voltage relationships with Q_{max} normalized to 1 and fitted to the Boltzmann equation: (▼) $V_{0.5} = -8 \pm 6$ mV for A166C, (○) $V_{0.5} = -24 \pm 7$ mV for A166C/MTSEA, and (●) $V_{0.5} = -50$ mV for A166C/MTSET. z was ≈1 for all three fits. (B) τ/voltage relationships of A166C (▼) ($\tau_{max} = 5.5$ ms), A166C/MTSEA (○) ($\tau_{max} = 3.7$ ms), and A166C/MTSET (●) ($\tau_{max} = 1.5$ ms).

Although the steady-state sugar-induced current was markedly inhibited after treatment with MTSET and MTSEA, the pre-steady-state charge movements were observed in saturating sugar (100 mM). After treatment with MTS reagents, there were minor changes in the pre-steady-state kinetics (in sugar) compared to the currents before treatment. Table 1 shows an example of an analysis of the pre-steady-state kinetics from one oocyte treated with MTSEA (1 mM for 2 min, at −50 mV). In α-MDG or D-Glu (100 mM), there was an increase in Q_{+50} ($Q_{+50}^{\alpha-MDG}$ from 6 to 13 nC and Q_{+50}^{D-Glu} from 6 to 14 nC) and τ_{+50} was the same (20 ms). In D-Gal, Q_{+50} was unchanged (11 nC before and 14 nC after) whereas τ_{+50} decreased slightly (20 ms before and 11−14 ms after). Both Q_{+50} and τ_{+50} were independent of pH. We

Table 1: Summary of the Pre-Steady-State Kinetics in Various Sugars[a]

	A166C		A166C/MTSEA	
	Q_{+50} (nC)	τ_{+50} (ms)	Q_{+50} (nC)	τ_{+50} (ms)
Na^+	27	5	19	3
α-MDG	6	20	13	20
D-Glu	6	20	14	20
D-Gal	11	20	14	12

[a] The experiments were performed on the same oocyte with the membrane potential held at −50 mV and then stepped to +50 mV. The external medium was NaCl buffer (pH 7.4) without or with 100 mM α-MDG, D-Glu, or D-Gal. The first and second columns show data obtained from A166C before treatment with MTSEA and the third and fourth columns the corresponding data after MTSEA treatment.

also examined pre-steady-state currents in A166C after labeling with MTSET, and found that the effect of MTSET was similar to that of MTSEA (not show).

DISCUSSION

These studies show that mutating residue 166 of hSGLT1 from an alanine to a cystine produces dramatic changes in the sugar selectivity and transport rate of the Na^+/glucose cotransporter. Furthermore, alkylating A166C with positively charged MTS reagents prevents sugar transport, but not sugar binding. This effect is due to the addition of a positively charged group at position 166, since (i) the inhibition by MTSEA was reversed by deprotonating the residue and (ii) treatment with a negatively charged reagent, MTSES, had no effect on sugar transport. In contrast, the effect of MTS reagents on A166C pre-steady-state kinetics was independent of the charge on the reagent and the pH of the assay. There are 15 cysteine residues in the native transporter, but these were unaffected by excess MTS reagents (this work and ref *14*). While many of our results confirm those initially reported by Silverman's group on A166C rabbit SGLT1 (*8*, *9*, *11*), our additional experiments lead us to a different interpretation. We propose that the residue at position 166 interacts with the sugar binding and translocating pathway of the protein, to determine the specificity and rate of sugar transport; changing the side chain of this residue results in a modification of the Na^+-involved conformational changes in the sugar binding/translocation pathway.

Comparison of A166C with WT SGLT1. Mutation of residue 166 from alanine to cysteine altered the substrate specificity and kinetics of hSGLT1. For WT, I_{max} was the same for D-Glu, D-Gal, and α-MDG, and $K_{0.5}^{sugar}$ was identical for the three sugars (0.2−0.3 mM) (*19*). In A166C, the values I_{max} and $K_{0.5}^{sugar}$ were in the following order: I^{D-Gal} (1) > I^{D-Glu} (0.8) > $I^{\alpha-MDG}$ (0.2) and $K_{0.5}^{D-Gal}$ (5.5 mM) > $K_{0.5}^{D-Glu}$ (1.5 mM) ∼ $K_{0.5}^{\alpha-MDG}$ (1.7 mM). Thus, the change in the maximal transport rate (I_{max}) was not related to a change in the affinity for sugar ($K_{0.5}^{sugar}$). The turnover number of each cotransporter is obtained by dividing the maximal Na^+/glucose current (I_{max} at −150 mV) by the maximal change (Q_{max}) (*14*, *20*). For A166C, the turnover numbers are 9.4 ± 0.6 s^{-1} for D-Gal, 8.7 ± 0.6 s^{-1} for D-Glu, and 2.1 ± 0.3 s^{-1} for α-MDG. In WT, the turnover number is 50 s^{-1} (*7*, *14*) and is the same for the three sugars (*7*, *19*, *21*). Thus, mutation of A166 to a cysteine results in a reduction in the turnover number compared to that of WT, as well as dependence of the turnover number on the sugar.

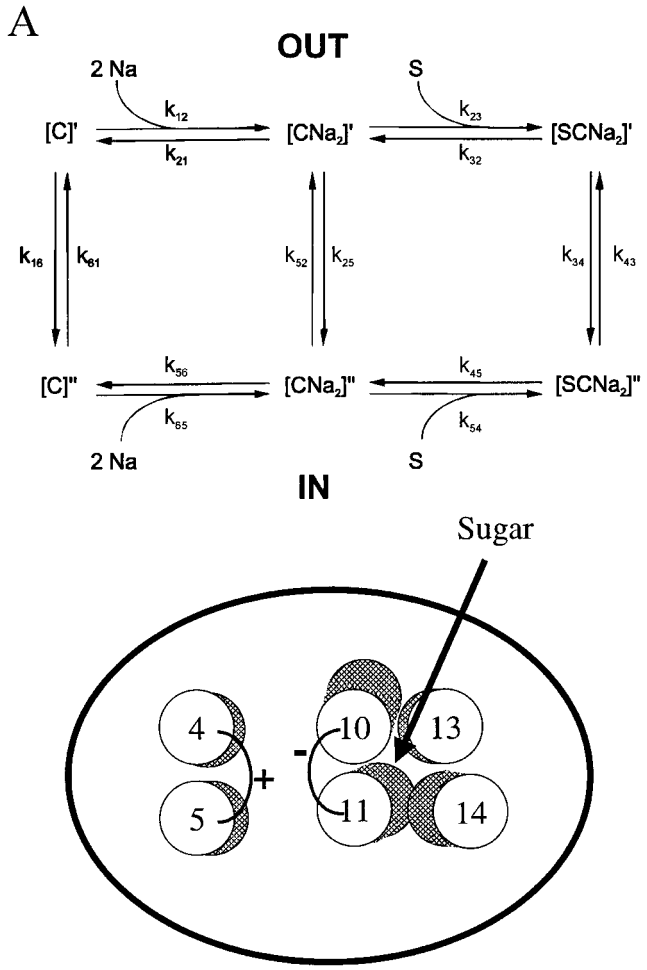

FIGURE 6: (A) Scheme illustrating the six-state ordered kinetic model for SGLT1 (modified from ref *22*). States C1 and C6, states C2 and C5, and states C3 and C4 represent the empty, Na^+-bound, and Na^+- and sugar-bound conformations ([C], [CNa_2], and [$SCNa_2$], respectively) of the transporter in the external and internal membrane surfaces. Two Na^+ ions bind to the transporter before the binding of one sugar molecule. k_{ij} represents the rate constant for the transition from state C*i* to C*j*. The pre-steady-state currents are due to the partial reactions C2 ⇆ C1 ⇆ C6. Sugar transport involves the partial reactions C3 ⇆ C4 ⇆ C5. The Na^+ leak current (Na^+ uniport) involves the reaction C2 ⇆ C5. (B) A cartoon illustrating the functional role of residue 166 (represented by the positive charge), situated between TMS 4 and 5, and the putative sugar binding/translocation pathway consisting of TMS 10−13 (*6*). Residue 166 modulates sugar recognition and binding as well as the conformational changes involved in sugar transport. The conserved D454 in the extracellular loop between TMS 10 and 11 is represented by the negative charge.

In contrast to the loss of affinity for sugars (in A166C compared to WT), there was a small increase in the apparent affinity for Na^+; at −150 mV, $K_{0.5}^{Na}$ was 0.9 ± 0.02 mM for A166C and 2.5 ± 0.1 mM for WT (*7*).

The kinetics of Na^+/glucose cotransport can be described by a six-state ordered kinetic model (*22*), and is illustrated in Figure 6A. The protein has six kinetic states, consisting of the empty transporter [C] [external (C1) and internal (C6)], the Na^+-bound transporter [CNa_2] [external (C2) and internal (C5)], and the sugar-bound transporter (CNa_2S) [external (C3) and internal (C4)]. Binding of Na^+ and sugar to the transporter is ordered with the Na^+ ions binding first. After Na^+ is bound, conformational changes result in an increase in the affinity of the transporter for sugar. When sugar binds, the transporter undergoes another conformational change and

the ligand binding sites become accessible to the intracellular membrane surface where the substrates are released and the empty ligand-binding sites return to the external membrane surface.

The pre-steady-state kinetics depend, in part, on Na^+ binding to the transporter, and we would expect that they would be affected by the mutation (*14*, *22*). Compared to that of WT, in A166C $V_{0.5}$ was shifted to more depolarizing potentials (≈30 mV, from −36 to −8, Figure 4B), and there was an increase in the rate of the transient current relaxations (Figure 4C). Pre-steady-state currents were also observed in saturating concentrations of sugar in A166C. This is in contrast to hSGLT1, where the pre-steady-state currents are abolished in the presence of saturating sugar concentrations (*1*).

The pre-steady-state currents are associated with binding/dissociation of Na^+ to the transporter (C2 ⇆ C1) on the external membrane surface and reorientation of the empty transporter from one side of the membrane to the other (C1 ⇆ C6). From the dependence of the transient currents on the rate constants k_{12}, k_{21}, k_{16}, k_{61} (see Figure 7 of ref *23*), an increase in the rate constant (k_{61}) of the conformational change from the internal to the external membrane surface could account for the differences in the pre-steady-state kinetics (in Na^+ buffer) between WT and A166C. An increase in k_{61} would result in (i) an decrease in τ_{max} (Figure 3D), (ii) a shift of $V_{0.5}$ to more positive values (Figure 3D), and (iii) an apparent increase in the affinity for Na^+ (see the Results).

The partial reactions involved in sugar translocation are: C3 → C4 → C5 → C6. For hSGLT1, these are voltage-independent, and at large negative potentials (e.g., at −100 mV), the rate-limiting step for sugar transport is k_{56} (*22*). In WT, the pre-steady-state currents are abolished in saturating concentrations of sugar. The kinetic model accounts for this observation, since in the presence of saturating sugar, most of the transporters are in the C5 conformation (*14*, *22*, *23*). In A166C, the pre-steady-state currents were observed in saturating sugar. Together with the reduction in the turnover rate for A166C, this indicates that the rate constant k_{34} and/or k_{45} is dramatically reduced, and now is the rate-limiting step for sugar transport. This conclusion also accounts for the charge movement observed in the presence of sugar, since a reduction in k_{34} (and/or k_{45}) would result in an accumulation of the mutant in the C3 conformation in the presence of sugar. From charge movement at +50 mV (Q_{+50}) (which was in the order $Q_{+50}^{D-Gal} > Q_{+50}^{\alpha-MDG} \cong Q_{+50}^{D-Glu}$) and the order of the $K_{0.5}$ values (see above; $K_{0.5}^{D-Gal} > K_{0.5}^{D-Glu} \approx K_{0.5}^{\alpha-MDG}$), we see that the higher the affinity for sugar, the more positive the $V_{0.5}$.

Effect of Alkylating Reagents on A166C. There were two functional effects on A166C after MTS modification: (i) an alteration in the pre-steady-state kinetics and (ii) an inhibition of Na^+/sugar cotransport. The latter was dependent, while the former was independent, of the charge of the MTS reagent. All three MTS reagents exerted similar effects on the pre-steady-state kinetics. The *Q*/*V* curve shifted along the *V*-axis to more hyperpolarizing values, and the relaxation kinetics became faster after C166 was modified (Figure 5). In addition, there was also a slight decrease in Na^+ affinity when it was determined after treatment with MTSEA at pH 9.0 (from 0.8 to 1.7 mM at −150 mV). The change in the time constant of the pre-steady-state current relaxation and the decrease in the apparent Na^+ affinity can be explained by an increase in the rate constant k_{16} of the conformational change from the external to the internal membrane surface (shifts $V_{0.5}$ to the left and decreases τ) (*23*).

The effect of alkylation by the MTS reagents was critically dependent on the charge of the reagent. This conclusion is based on the findings that (i) the negatively charged MTS reagent (MTSES) reacts with the transporter [perturbs pre-steady-state kinetics (Figure 5)] but does not inhibit Na^+/sugar cotransport, (ii) positively charged MTS reagents [MTSEA (pH. 7.5) and MTSET] both perturb pre-steady-state kinetics and block Na^+/sugar cotransport (Figures 4A and 5), (iii) by neutralizing the positive charge on MTSEA (increase the pH to 9.0) Na^+/sugar cotransport is recovered (Figure 4A), (iv) the pre-steady-state kinetics in A166C alkylated with MTSEA are independent of pH, and (v) pre-steady-state charge movement, after labeling with all reagents, is influenced by sugar, indicating that sugar interacts with the transporter. Since uptake studies showed directly that there is no sugar uptake after MTSET treatment, this indicates that kinetically, the rate constant k_{34} and/or k_{45} is reduced to zero by the positively charged MTS reagents.

In summary, compared to those of WT, the change in kinetics of A166C can be attributed to (i) an increase in the rate constant k_{61} for the conformational change of the empty transporter from the internal to the external membrane surface, (ii) a decrease in the K_D for sugar ($=k_{23}/k_{32}$), and (iii) a sugar-dependent decrease in the rate constants k_{34} and/or k_{45} of the sugar translocation step. After alkylation of A166C by positively charged MTS reagents, there was (i) an increase in k_{16} and (ii) a decrease of k_{34} or k_{45} to 0; i.e., Na^+-dependent sugar transport was abolished, but only if the MTS reagent was positively charged.

Functional Role of Residue 166. It has been found that mutations of residues in the N-terminus of a number of cotransporters result in changes in the specificity and affinity for cations. In human SGLT1, replacement of Asp^{204} with Glu, Asn, or Cys primarily resulted in changes in the affinity and specificity for cations (Na^+ and H^+) (*7*). The Na^+/proline permease from *Escherichia coli* (PutP) belongs to the SGLT family of transport proteins, and it has been shown that Asp 55 in the N-terminus is essential for Na^+ binding (*24*). In A166C, we found a slight increase in the apparent affinity of the mutant for Na^+.

Since A166C was readily labeled by the impermeant MTS reagents (MTSET and MTSES) from the external membrane surface, residue 166 must be on the external membrane surface. In addition, there was no effect of membrane voltage on the rate of labeling by the MTS reagents, nor an effect on pre-steady-state charge movement with different charged reagents, indicating that the residue is located beyond the membrane electric field on the external membrane surface. These findings are consistent with the 14 TMS model (*3*).

It has been shown that accessibility of residues in the sugar (binding/translocation) pathway of hSGLT1 is dependent on the conformational state of the protein, and is controlled by the external substrate concentrations and membrane voltage (*2*). An example is residue C457, which is accessible to MTS reagents from the external membrane surface in the presence of Na^+ and at negative membrane potentials, and is protected from alkylation in the presence of sugar and phlorizin (*2*). Residue 166 does not appear to be in the sugar (binding/translocation) pathway, because accessibility of MTS reagents to C166 from the external membrane surface was not influenced by Na^+, sugar, phlorizin, or membrane voltage.

However, the residue seems to be "functionally" close to the sugar pathway in view of the alteration in the sugar specificity of A166C compared to that of WT. The change in $K_{0.5}$ for sugar could be due to a local change in the sugar-binding pocket where it interacts with the OH group at position 4 of the sugar, which is the only difference between D-Glu (equatorial OH group) and D-Gal (axial OH group). The proximity of residue C166 to the sugar pathway is consistent with the cross-linking studies on *Vibrio parahaemolyticus* vSGLT1, which indicates that the extracellular loop between putative TMS 4 and 5 is within 8 Å of the sugar pathway (*12*).

We envision the effect of mutating residue 166 from alanine to cysteine as follows: (i) Na^+ binding is not affected, and the conformational change induced in the Na^+ pathway proceeds normally. The information that is conveyed to the sugar-binding pathway is inaccurately transmitted (C2 → C3). This results in an alteration in the shape of the sugar-binding pathway, as evidenced by the reduced affinity of D-Gal relative to those of D-Glu and α-MDG. (ii) Our kinetic model also implies that the binding of the sugar triggers another conformational change (C3 → C4 → C5) in the protein, which results in the reorientation of the binding site to the interior surface of the membrane and Na^+/sugar cotransport. In the case of C166, the interaction with the OH group at pyranose position 1 is critical. D-Glu and D-Gal are transported with the same maximal velocity (I_{max}), albeit with different affinities; if a methyl group is added to the glycosidic oxygen (α-MDG), the I_{max} is reduced 5-fold, although the affinity is high, suggesting that the conformational change triggered by the sugar is inefficient.

Alkylation of residue 166 did not cause a significant alteration in the sugar binding site. However, the fact that binding of a positively charged reagent prevents translocation suggests a direct interaction with a nearby negatively charged residue (Figure 6B). A candidate for this interaction is a highly conserved aspartate residue (D454 in hSGLT1) located in the loop between TMS 10 and 11 (*3*). Electrostatic repulsion between $MTSES^-$ and the negative charge does not seem to have an effect on sugar transport. Currently, the involvement of residue 454 is being tested by mutagenesis of D454 to cysteine and histidine.

Lo and Silverman (*8*, *9*) have analyzed A166C in rabbit SGLT1. Both human and rabbit A166C show no change in Na^+ affinity, but do exhibit a decrease in sugar (α-MDG) affinity compared to that of WT. We have extended these observations by showing that the most profound effect on the kinetic properties is a reduction in the turnover rate, and this depends on the sugar, as well as the charge on residue 166. In the hSGLT1 mutation, the pre-steady-state charge movements are observed in the presence of sugar, whereas it is not in the rSGLT1 mutant (*8*, *9*). While we propose that residue 166 is important for the interaction between the Na^+ and sugar pathways, the conclusion of Lo and Silverman is that residue 166 is directly involved in Na^+ binding (*8*, *9*).

Our conclusion that residues at position 166 of SGLT1 are involved in interactions that modify sugar turnover is similar to that of a recent study on the melibiose permease from *E. coli* (MelB) of tryptophans located in and around TMS 4 (*25*). This cotransporter exhibits many functional similarities to SGLT1 such as the specificity to Na^+, H^+, and Li^+ and the relationship between the $K_{0.5}$ and I_{max} for Na^+ and the sugar substrate (*26*, *27*).

ACKNOWLEDGMENT

We thank Daisy W. Leung and Mary L. Bing for the preparation and injection of oocytes, and Jason Lam for the construction of the A166C mutation.

REFERENCES

1. Parent, L., Supplisson, S., Loo, D. D. F., and Wright, E. M. (1992) *J. Membr. Biol. 25*, 49−62.
2. Loo, D. D. F., Hirayama, B. A., Gallardo, E. M., Lam, J. T., Turk, E., and Wright, E. M. (1998) *Proc. Natl. Acad. Sci. U.S.A. 95*, 7789−7794.
3. Turk, E., and Wright, E. M. (1997) *J. Membr. Biol. 159*, 1−20.
4. Eskandari, S., Wright, E. M., Kreman, M., Starace, D. M., and Zampighi, G. A. (1998) *Proc. Natl. Acad. Sci. U.S.A. 95*, 11235−11240.
5. Panayotova-Heiermann, M., Loo, D. D. F., Kong, C. T., Lever, J. E., and Wright, E. M. (1996) *J. Biol. Chem. 271*, 10029−10034.
6. Panayotova-Heiermann, M., Eskandari, S., Turk, E., Zampighi, G. A., and Wright, E. M. (1997) *J. Biol. Chem. 272*, 20324−20327.
7. Quick, M., Loo, D. D. F., and Wright, E. M. (2001) *J. Biol. Chem. 276*, 1728−1734.
8. Lo, B., and Silverman, M. (1998) *J. Biol. Chem. 273*, 903−909.
9. Lo, B., and Silverman, M. (1998) *J. Biol. Chem. 273*, 29341−29351.
10. Martin, M. G., Turk, E., Lostao, M. P., Kerner, C., and Wright, E. M. (1996) *Nat. Genet. 12*, 216−220.
11. Vayro, S., Lo, B., and Silverman, M. (1998) *Biochem. J. 332*, 119−125.
12. Xie, Z., Turk, E., and Wright, E. M. (2000) *J. Biol. Chem. 275*, 25959−25964.
13. Ho, S. N., Hunt, H. D., Horton, R. M., Pullen, J. K., and Pease, L. R. (1989) *Gene 77*, 51−59.
14. Loo, D. D. F., Hazama, A., Supplisson, S., Turk, E., and Wright, E. M. (1996) *Proc. Natl. Acad. Sci. U.S.A. 90*, 5767−5771.
15. Ikeda, T. S., Hwang, E. S., Coady, M. J., Hirayama, B. A., Hediger, M. A., and Wright, E. M. (1989) *J. Membr. Biol. 110*, 87−95.
16. Karlin, A., and Akabas, M. H. (1998) *Methods Enzymol. 293*, 123−145.
17. Mackenzie, B., Loo, D. D. F., and Wright, E. M. (1998) *J. Membr. Biol. 162*, 101−106.
18. Diez-Sampedro, A., Eskandari, S., Wright, E. M., and Hirayama, B. A. (2001) *Am. J. Physiol. 49*, F278−F282.
19. Diez-Sampedro, A., Lostao, M. P., Hirayama, B. A., and Wright, E. M. (2000) *J. Membr. Biol. 176*, 111−117.
20. Zampighi, G. A., Kreman, M., Boorer, K. J., Loo, D. D. F., Bezanilla, F., Chandy, G., Hall, J. E., and Wright, E. M. (1995) *J. Membr. Biol. 148*, 65−78.
21. Birnir, B., Loo, D. D. F., and Wright, E. M. (1991) *Pfluegers Arch. 418*, 79−85.
22. Parent, L., Supplisson, S., Loo, D. D. F., and Wright, E. M. (1992) *J. Membr. Biol. 25*, 63−79.
23. Hazama, A., Loo, D. D. F., and Wright, E. M. (1997) *J. Membr. Biol. 155*, 175−186.
24. Quick, M., and Jung, H. (1997) *Biochemistry 36*, 4631−4636.
25. Cordat, E., Leblanc, G., and Mus-Veteau, I. (2000) *Biochemistry 39*, 4493−4499.
26. Hirayama, B. A., Loo, D. D. F., and Wright, E. M. (1997) *J. Biol. Chem. 272*, 2110−2115.
27. Pourcher, T., Bassilana, M., Sarkar, H. K., Kaback, H. R., and Leblanc, G. (1990) *Philos. Trans. R. Soc. London, Ser. B 326*, 411−423.

BI011026L